JOURNAL OF MATERIALS SCIENCE 24 (1989) 183–186

Double necking in polymer tensile deformation

ERWIN PINK, ANDREAS KRONTHALER*, PETRA VALTINGOIER
Erich-Schmid-Institut für Festkörperphysik der Österreichischen Akademie der Wissenschaften, Leoben, Austria

After initial necking of tensile polymer samples the deformation front moves along the gauge length at a stress which is smaller than the yield stress. The still "undeformed" parts of the sample are therefore subjected to conditions which favour deformation by a creep mechanism. If the extension rate is right, secondary necking becomes possible. Boundary conditions are discussed.

1. Introduction

A neck in a polymer, once formed in tensile deformation, does not immediately lead to fracture. It is the starting point for the deformation front to propagate, so that extensions up to several 100% can be attained. It is well known that, while this front propagates, a second neck can form in the apparently undeformed parts of the sample.

It will be shown that this secondary necking is a necessary consequence of the testing conditions, and not caused by accidental weakening in some disturbed spots. Fig. 1 is an example of how some polymers deform in tensile tests. After the yield point (defined as the maximum load which is approximately also the maximum stress) the load drops until the neck assumes its largest extent. Then the deformation front propagates while the applied load remains constant. Those parts of the sample, which are ahead of the deformation front and still "undeformed", experience a stress, which is determined by the constant load at which the front propagates. We propose that creep deformation sets in here, leading to another necking if there is sufficient time.

To investigate this possibility, it is necessary to conduct tensile tests as well as creep tests at stresses similar to the propagation stress of the front. The following materials were investigated: PVC "Trovidur" of Dynamit - Nobel, the PP-based "Daplen PPHO 50" of Chemie Linz, and PMMA of unknown source.

2. The tensile tests

Tensile tests were carried out with samples of 5 mm diameter and 25 mm gauge length at various crosshead velocities v_{CH}. Fig. 1 shows examples from tensile testing of the three materials. Values of the yield stresses σ_y (defined as the stress at the point of maximum load related to the initial diameter D_0) and the "front-propagation" stresses σ_p (again related to D_0) are listed in Table I together with the ratios d_i/D_0 (d_i is the average diameter of those sample portions which the deformation front has already passed)†. σ_p is not significantly changed during the tests as the sample length increases, and thus the true strain rate decreases. Also indicated in the table is the tendency of the materials to form secondary necks.

3. The creep tests

Creep tests were conducted at room temperature on a tensile-testing machine. A function generator allowed the load to be kept constant which means that the applied stress is, to a first approximation, constant until necking begins after a time t_N (see insert in Fig. 2). In the range II (according to the schematic picture) the extension rate is constant, and it is constant again after t_P, the time when front propagation sets in (range IV).

Fig. 2 gives results from the creep tests. The time t_N for the start of necking is plotted as a function of the applied stress which is normalized in order to allow comparison of the different materials: the creep stress σ_c is chosen in relation to the material characteristics σ_y and σ_P, below as well as above σ_P. Note the difference between the curves for PVC: one stems from

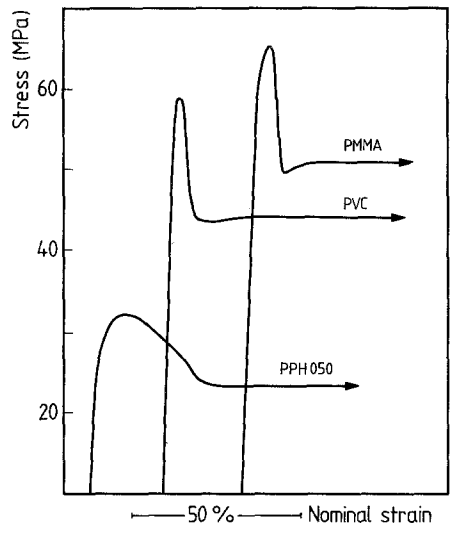

Figure 1 Yielding of three polymeric materials: the stress in the "undeformed" parts of the sample gauge. Gauge length = 25 mm, v_{CH} = 1 mm min^{-1}, room temperature.

Present address: RADEX Austria A.G., Vienna, Austria.
†The reduced diameter d_i varies with material: it is apparently proportional to the yield stress σ_y of the material (see Table I).

0022–2461/89 $03.00 + .12

TABLE I Characteristics of tensile deformation at room temperature, at $v_{CH} = 1\,mm\,min^{-1}$.

Material	PVC Trovidur	PPHO50 Daplen	PMMA
σ_y(MPa)	57–60	31–32	66–68
σ_p(MPa)	41–44	23–24	51–54
d_i/D_0	0.65–0.68	0.45–0.48	0.78
Double necking	"New": GL = 25 mm NO GL = 50 mm YES "Aged": GL = 50 mm NO	"Aged": GL = 50 mm YES (fast!)	"Aged": GL = 50 mm NO

*GL is the gauge length.

tests with the "fresh" material, the other one from PVC which was aged at room temperature for about ten years. Although their creep behaviour is significantly different, no influence was exerted on σ_y and σ_P (see Table I).

The data points for t_N in the diagram are connected by a curved line. This curvature of the stress dependence of t_N comes about through the parameters of thermally activated deformation [1] and has been theoretically explained as an inherent property [1–3] or as stemming from an interaction of two deformation mechanisms [4, 5].

4. Neck formation and front propagation in tensile tests

A primary neck may develop somewhere in the middle of the gauge length or, due to insufficiently accurate aligning and stress concentrations, also on either end of the gauge close to the sample head. The deformation front propagates then either in the direction of the cross head or in the opposite direction. This is schematically sketched in Fig. 3.

The progress of the primary deformation front in tensile tests is of interest for judging whether a secondary neck has the opportunity to develop. In our tests,

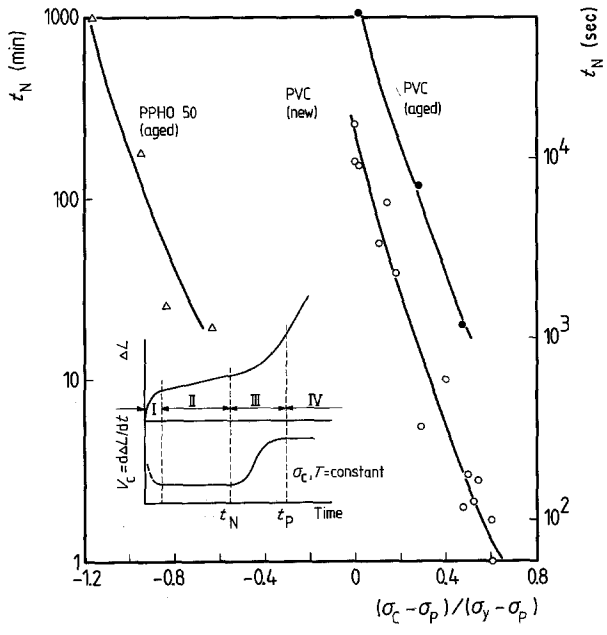

Figure 2 The dependence of the time t_N (when necking starts in creep tests) on the creep stress σ_c for different materials at room temperature.

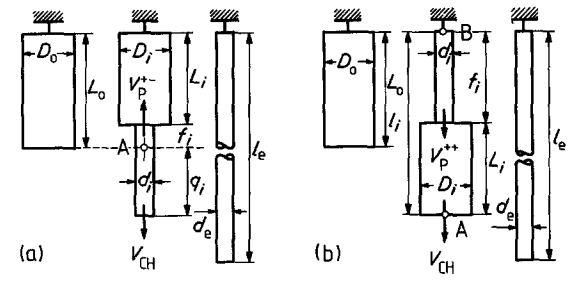

Figure 3 Schematic representation of the front propagation starting at (a) the lower and (b) the upper end of the gauge length.

the propagation was registered by photographic means, and measured on a screen from the enlarged projection of the negative film.

Fig. 4 demonstrates the progress of the front f_i (defined as all other symbols in Fig. 3) as a function of time for different cross-head velocities v_{CH} (zero time was chosen arbitrarily after primary necking had reduced the diameter D_i to its minimum value d_i).

Independent of whether primary necks develop on the upper or lower end of the sample, the deformation front propagates at a velocity v_P either in the same (++) or in the opposite (+−) direction of the cross-head

$$v_{P,A}^{+-} = v_{P,A}^{++} = v_{CH}/K_i \qquad (1)$$

where $K_i = (D_i/d_i)^2 - 1$. Position A (stationary with respect to the undeformed sample ends) according to Fig. 3 is the points of reference. We assumed constant volume during deformation in order to derive Equation 1. In the case of front and cross head moving in opposite directions (Fig. 3a), the equation was derived by defining

$$v_{P,A}^{+-} = \frac{df_i}{dt} \quad v_{CH} = \frac{dq_i}{dt} = \frac{d(q_i + L_0)}{dt} \qquad (2)$$

For front and cross head moving in the same direction (Fig. 3b) we defined

$$v_{P,A}^{++} = \frac{dL_i}{dt} \quad v_{CH} = \frac{dl_i}{dt} \qquad (3)$$

For B as the reference point according to Fig. 3b, the

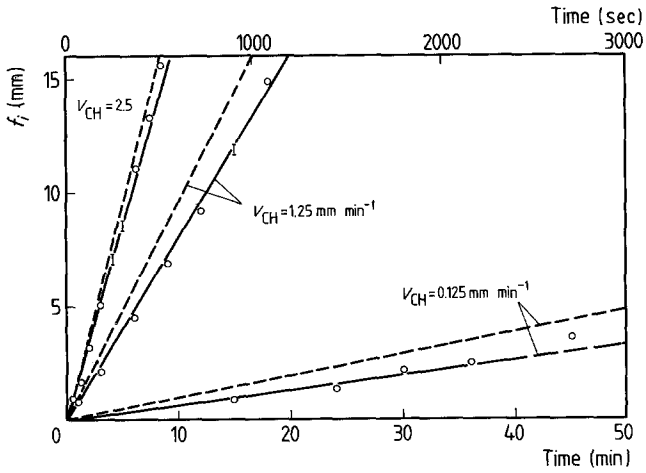

Figure 4 Experimental and calculated progress of deformation fronts (the case of Fig. 3a). PVC (new) 25° C, D_0 = 5 mm, d_i = 3.3 mm, —o— experimental, ---- calculated.

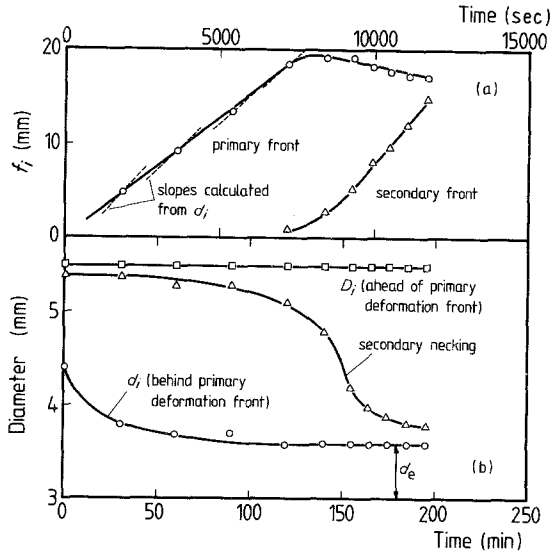

Figure 5 (a) Propagation of the primary and secondary front, (b) the development of the secondary neck. PVC (new) 25° C, v_{CH} = 0.25 mm min^{-1}.

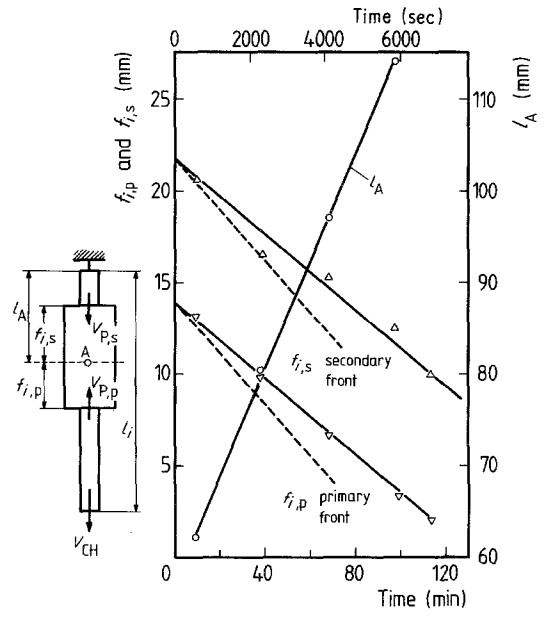

Figure 6 The propagation of primary and secondary deformation fronts in relation to position A, and the translation of position A. PPHO 50 (aged), v_{CH} = 1 mm min^{-1}, D_0 = 6 mm, d_i = 2.8 mm, – – – – calculation.

results are different. We defined

$$v_{P,B}^{++} = \frac{df_i}{dt} \quad v_{CH} = \frac{dl_i}{dt} \tag{4}$$

which leads to

$$v_{P,B}^{++} = v_{CH}\,(K_i + 1)/K_i \tag{5}$$

This illustrates the obvious fact that the deformation front must propagate at a faster rate than the cross head when both speeds are related to the sample end B.

The situations depicted in Fig. 3 are of course identical, since A in Fig. 3a is equally suited as is a reference point at the undeformed end of the sample, i.e. as point A in Fig. 3b, which is proved by Equation 1. Neither is there any fundamental difference between the points A and B in Fig. 3b. Whether we measure the distance f_i between front and B, instead of the distance L_i between front and A, is rather a question of convenience.

Equations 1 and 5 naturally are idealizations because the quantities D_i and d_i are supposed to be constant during deformation, and also in every part of the sample. We still, despite the further simplification that $D_i = D_0$ and $d_i = d_e$, obtain reasonable agreement with the experiments as seen in Fig. 4 (the case of Fig. 3a). The deviations can be explained in part by the creep deformation of the "still undeformed" portions of the sample which retards the front propagation.

Fig. 5 demonstrates the case of double necking. The time scale with its arbitrarily chosen origin begins close to the end of primary-neck formation, and continues beyond the point where secondary necking has started. In Fig. 5b we see how the initial $D_i \approx D_0$ is, in the centre of necking, gradually constricted toward the value d_i, and how d_i in the wake of the primary neck approaches d_e. When the secondary neck appears, the primary front recedes (Fig. 5a), because the progress of both fronts has been related to the upper fixed end of the sample (which is equivalent to relating to point A of Fig. 3a).

A better point of reference is that used in the diagram of Fig. 6, because it allows the immediate determination of both front velocities. Point A is chosen to remain situated within the "still undeformed" part even when primary (index p) and secondary (index s) fronts both move. Velocities can be defined as

$$v_{P,s}^{++} = v_{P,s,A} = \frac{df_{i,s}}{dt} \quad v_{P,p}^{+-} = v_{P,p,A} = \frac{df_{i,p}}{dt}$$

$$v_{CH} = \frac{dl_i}{dt} \tag{6}$$

$v_{P,s}$ is the velocity of the front emanating from the secondary neck. $f_{i,s}$ and $f_{i,p}$ decrease as the fronts propagate. The experimental velocities of both fronts in Fig. 6 are ~0.1 mm min^{-1}. By means of Equation 1 it can be calculated that a single front should travel with 0.28 mm min^{-1}. Taking into account that there are two fronts (and that both their experimental velocities are equal), we may well assume half the value, i.e. 0.14 mm min^{-1}, as the speed calculated for a single front. Such progress is indicated by the dashed lines. The deviations from reality are again of the same magnitude as those in Fig. 4.

5. Discussion

The goal is to prove that secondary necking is caused by creep deformation. For a front-propagation stress σ_P = 41 MPa (see Table I) the time t_N until necking in PVC (new) is, according to Fig. 2, 160–270 min. Thus, for a gauge length of 25 mm, there is never an opportunity for secondary necking in the two fast tests of Fig. 4, because the primary front has reached the sample end in times shorter than t_N. Indeed fast tests never did lead to double necking.

The slower the test, the better are the chances for secondary necking. However, since the sites of necking are determined by "accident", a secondary neck could start to form in the vicinity of the approaching primary

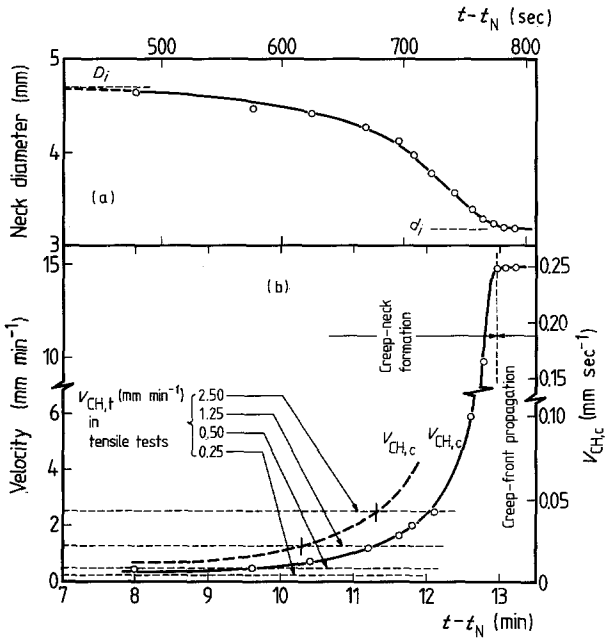

Figure 7 The neck formation in creep at a creep stress σ_c equal to the front-propagation stress σ_p (a) the reduction of the neck diameter, (b) the cross-head velocity $v_{CH,c}$ in the creep test, related to several tensile-test cross-head velocities. PVC (new) 25° C, σ_c = 41 MPa (nominal stress).

front, and be swallowed by it. Increasing the length of the sample may provide better chances.

There is a discrepancy between t_N of PVC for σ_c = 41 MPa (Fig. 2) and the time in Fig. 5, when the secondary neck starts forming. This has a two-fold explanation. The lesser influence comes from the fact, mentioned earlier, that the origin was arbitrarily chosen only some time after the primary-neck diameter had assumed some value d_i. The more important influence comes from the fact that in tensile tests all parts within the gauge length have been exposed during yielding to stresses higher than σ_p. This must accelerate the creep process. As Fig. 1 shows, the yield process consumes different times depending on the material: for PPHO 50 it lasts a long time. Indeed the formation of secondary necks is fastest in PPHO 50. That secondary necks appear easily in PPHO 50 has also another explanation: according to Fig. 2, the creep rate is high even when the applied creep stresses σ_c are lower than σ_p.

We have concluded that a low strain rate favours the formation of a secondary neck. However, there is a boundary condition which later, during secondary necking, has just the reverse effect. In a true creep test, the creep velocity and thus $v_{CH,c}$ (which is controlled by the function generator) increases rapidly with time when the sample necks. In a tensile test such a free creep deformation of the "undeformed" part will be partly obstructed. This is explored in Fig. 7 with the help of the extension velocity (i.e. $v_{CH,c}$). The obstruction of creep necking begins when this velocity $v_{CH,c}$ matches the extension velocity of the "undeformed" (i.e. creeping) sample parts. However, when a secondary neck forms in a tensile test, the extension rate of the hitherto "undeformed" material is not determined by the cross head speed $v_{CH,t}$, but it is diminished due to the existence of the primary front by almost 50% (c.f. the slope dl_A/dt = 0.58 mm min^{-1} in Fig. 6 for v_{CH} = 1 mm min^{-1}). The crossing point of such a speed ($v_{CH,t}/2$) with $v_{CH,c}$ is the limit, from which on the creep-neck formation should be obstructed. For the sake of better clarity we used, in Fig. 7b, a curve $v'_{CH,c}$, twice as high as $v_{CH,c}$, and looked where it crosses the $v_{CH,t}$ levels (instead of decreasing the $v_{CH,t}$ values by a factor of 2 and comparing them with $v_{CH,c}$). How deep the neck will be at this moment, is seen in Fig. 7a: for the low cross-head speeds secondary necks should hardly develop.

Thus there are two counterproductive effects.

(1) Slow tensile expansion rates improve the chances of secondary necks forming, but the maximum achievable reduction in neck diameter is minor.

(2) Fast tensile tests, which would allow the neck diameter to decrease markedly, do not provide the time necessary for secondary necks to be initiated.

The development of secondary necks is only possible within narrow limits of testing conditions. That they appear after all may be for the following reason: strain-hardening in incomplete necks may not yet be as severe as in fully formed deformation fronts, so deformation takes over at the nucleation site of the new, secondary neck. Later, when the secondary neck has attained the shape of a fully developed deformation front, both fronts are equally capable of propagating. A condition is now achieved which is depicted in Fig. 6.

References

1. E. PINK, A. KRONTHALER, *Materialprüfg.* **19** (1977) 201.
2. E. PINK, *Mater. Sci. Engng.* **22** (1976) 85.
3. B. ESCAIG and J. M. LEFEBVRE, *Rev. Phys. Appl.* **13** (1978) 285.
4. J. C. BAUWENS, *J. Mater. Sci.* **7** (1972) 577.
5. C. BAUWENS-CROWET, *ibid.* **8** (1973) 968.

Received 23 April 1987
and accepted 27 April 1988